Deep Learning Applications in Stroke Risk Assessment using B-mode Carotid Ultrasound Images

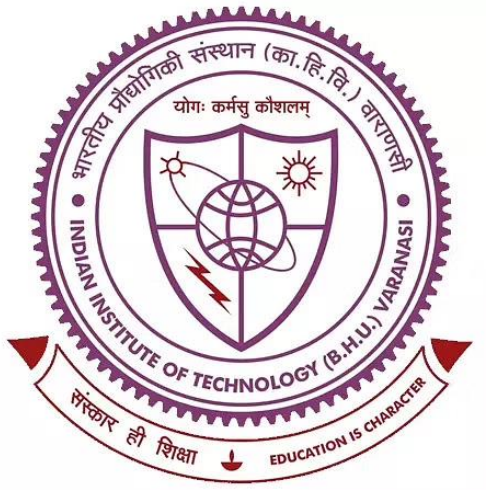

Thesis submitted in partial fulfilment for the
Award of Degree

Doctor of Philosophy

By
Pankaj Kumar Jain

SCHOOL OF BIOMEDICAL ENGINEERING
INDIAN INSTITUTE OF TECHNOLOGY
(BANARAS HINDU UNIVERSITY)
VARANASI – 221005
INDIA

ROLL NO: 17021504

2023

CERTIFICATE

It is certified that the work contained in the thesis titled "**Deep Learning Applications in Stroke Risk Assessment using B-mode Carotid Ultrasound Images**" by " ***Mr. Pankaj Kumar Jain*** " has been carried out under our supervision and that this work has not been submitted elsewhere for a degree.

It is further certified that the student has fulfilled all the requirements of Comprehensive Examination, Candidacy and SOTA for the award of Ph.D. Degree.

Neeraj Sharma
12/01/2023

Professor Neeraj Sharma
(Supervisor)
School of Biomedical Engineering
Indian Institute of Technology
(Banaras Hindu University)
Varanasi - 221005, (U.P.), India.

SUPERVISOR

Jasjit S. Suri

Digitally signed by Jasjit S. Suri
DN: cn=Jasjit S. Suri, o=AtheroPoint LLC, ou=Stroke Monitoring Division, email=Jasjit.Suri@AtheroPoint.com, c=US
Date: 2022.11.10 21:11:57 -08'00'

Professor Jasjit S Suri
(Co-Supervisor)
CEO, AtheroPoint LLP,
Roseville, CA, USA

DECLARATION BY THE CANDIDATE

I, ***Pankaj Kumar Jain,*** certify that the work embodied in this Ph.D. thesis is my own bonafide work and carried out by me under the supervision of ***Prof. Neeraj Sharma and Co-supervision of Prof. Jasjit S. Suri*** from "*27 July 2017*" to "*23 August 2022*" at **School of Biomedical Engineering, Indian Institute of Technology (BHU), Varanasi.** The matter embodied in this thesis has not been submitted for the award of any other degree/diploma. I declare that I have faithfully acknowledged and given credit to the research workers wherever their works have been cited in my work in this thesis. I further declare that, I have not wilfully copied any other's work, paragraphs, text, data, results, etc. reported in the journals, books, magazines, reports, dissertations, thesis, etc., or available at websites and have not included them in this Ph.D. thesis and have not cited as my own work.

Date: 12/01/2023

Place: IIT (BHU), Varanasi

Pankaj Jain

(Pankaj Kumar Jain)

CERTIFICATE BY THE SUPERVISOR

It is certified that the above statement made by the student is correct to the best of our knowledge.

Neeraj Sharma 12/01/2023

Professor Neeraj Sharma
(Supervisor)

Jasjit S. Suri

Digitally signed by Jasjit S. Suri
DN: cn=Jasjit S. Suri, o=AtheroPoint LLC, ou=Stroke Monitoring Division, email=Jasjit.Suri@AtheroPoint.com, c=US
Date: 2022.11.10 21:12:25 -08'00'

Professor Jasjit S Suri
(Co-supervisor)

SUPERVISOR

Signature of Head of Department/Coordinator of School
"SEAL OF THE DEPARTMENT/SCHOOL

समन्वयक/CO-ORDINATOR
जैव चिकित्सा अभियांत्रिकी स्कूल
SCHOOL OF BIOMEDICAL ENGG
भारतीय प्रौद्योगिकी संस्थान (का.हि.वि
INDIAN INSTITUTE OF TECHNOLOGY (B.H.U
वाराणसी-221005/VARANASI-221005

COPYRIGHT TRANSFER CERTIFICATE

Title of the Thesis: **Deep Learning Applications in Stroke Risk Assessment using B-mode Carotid Ultrasound Images**

Candidate's Name: Mr. Pankaj Kumar Jain

Copyright Transfer

The undersigned hereby assigns to the Indian Institute of Technology (Banaras Hindu University) Varanasi all rights under copyright that may exist in and for the above thesis submitted for the award of the "*DOCTOR OF PHILOSOPHY*".

Date: 12/01/2023

Place: Varanasi

Pankaj Kumar Jain

Note: However, the author may reproduce or authorize others to reproduce material extracted verbatim from the thesis or derivative of the thesis for author's personal use provided that the source and University's copyright notice are indicated.

ACKNOWLEDGEMENT

I would like to take this opportunity to thank all my acquaintances who helped me through this research journey. This thesis appears in its current form due to the assistance and guidance of many people. Therefore, I would like to thank all of them.

I would like to express my sincere gratitude to my supervisor, Professor Neeraj Sharma and co-supervisor, Professor Jasjit S. Suri, for granting me this research opportunity. Under their supervision, guidance, motivation, and encouragement, I can complete this work. I express my sincere thanks to my research progress evaluation committee members, Professor Rajeev Shrivastava and Dr Shiru Sharma. Their valuable suggestions, comments and constant support improved the quality of research work. I gratefully acknowledge Professor Prasun K. Roy, Dr Sanjay K Rai, Dr Sanjeev K Mahto, and Dr Pradeep Paik of the School for smoothing out all official documents. I would like to sincerely thank all the supporting staff of the School for their kind help whenever I required it.

I also thank Dr Arnav Bhavsar Associate Prof., Dr Aditya Nigam, and Assistant Prof. IIT Mandi (HP), Dr Bikesh Singh, Dr Narendra Londhe, Associate Prof., Dr Saurabh Gupta, Assistant Prof. NIT Raipur (CG), Dr Sumit Banchhor Faculty, NIT Raipur, Dr Vimal Shrivastava, Assistant Prof. KIIT Bhuwneshwer, for their support and guidance in medical imaging. My friends Prem Shankar Gupta, Nillmani, Sumit, Bindu, Kirti, Snehlata and Prateek who never left me alone.

Finally, I would like to thank my family for all their love, encouragement, and trust. I would like to express my sincere regards to my father, Shri Santosh Jain and father-in-law Surit Jain who supported me in all my pursuits. I would like to express my sincere thanks and love to my wife, Mrs Sonam Jain, for her unconditional love and support during this journey. She is always a source of inspiration for me. My son Mr Parikshit and daughter Siya always showed their love to me.

Thank you all.
Date : 12/01/2023
Place : Varanasi

(Pankaj Kumar Jain)

Dedicated to My Family

Table of Contents

S. No.	Description	Page No.
a)	List of Tables	x
b)	List of Figures	xii
c)	List of Abbreviations	xvii
d)	List of Symbols	xviii
e)	Preface	xx
1.0	**Chapter 1: Introduction**	**01**
1.1	Introduction	01
1.2	PRISMA Model and Article Search strategy	03
1.3	Plaque morphology	04
1.4	Carotid Artery Subsections and Biomarkers	05
1.5	Carotid Imaging Modalities	06
1.6	Discussion	07
1.7	Objectives of the Thesis	10
1.8	Thesis Organization	10
2.0	**CVD Risk Biomarkers: Automated Measurement and Quantification**	**11**
2.1	Historical Background	11
2.2	Generations of Segmentation Methods	11
2.3	Deep Learning in other Medical Imaging Applications	14
2.4	UNet Based Segmentation Model and Its Variants	14
2.5	Critical Remarks: Quantitative Assessment of Carotid Biomarker using Deep Learning	18
2.6	Hardware and Software for DL Systems	23
2.7	Biases in Deep learning Based Systems	23
2.8	Conclusions	23
3.0	**Hybrid Deep Learning Segmentation Models for Atherosclerotic Plaque in Internal Carotid Artery B-mode Ultrasound**	**24**
3.1	Introduction	24
3.2	Methodology: Data Preparation, AI Architectures, and Experimental Protocol	24

3.3	Experimental Protocol	33
3.4	Experimental Results	34
3.5	Performance Evaluation	36
3.6	Discussion	45
3.7	Conclusion	52
3.8	Proposed Extension	52
4.0	**Automated Deep Learning-Based Paradigm for High-Risk Plaque Detection in B-mode Common Carotid Ultrasound Scans: An Asymptomatic Japanese Cohort Study**	**53**
4.1	Introduction	53
4.2	Methodology	55
4.3	Experimental Results	61
4.4	Performance Evaluation and Statistical Tests	63
4.5	Discussion	73
4.6	Conclusion	73
4.7	Proposed Extension	73
5.0	**Unseen Artificial Intelligence–Deep Learning Paradigm for Segmentation of Low Atherosclerotic Plaque in Carotid Ultrasound: A Multicentre Cardiovascular Study**	**74**
5.1	Introduction	74
5.2	Methodology	77
5.3	Results	79
5.4	Performance Evaluation	81
5.5	Discussion	85
5.6	Conclusions	89
5.7	Proposed Extension	89
6.0	**Far Wall Plaque Segmentation and Area Measurement in Common and Internal Carotid Artery Ultrasound using U-Series Architectures: An Unseen Artificial Intelligence Paradigm for Stroke Risk Assessment**	**90**
6.1	Introduction	90
6.2	Demographics and data preparation	92
6.3	Methodology	93

6.4	Results	103
6.5	Performance Evaluations	106
6.6	Discussion	111
6.7	Conclusion	117
6.8	Proposed Extension	117
7.0	**Attention-Based UNet Deep learning model for Plaque Segmentation in Carotid Ultrasound for Stroke Risk Stratification: An Artificial Intelligence Paradigm**	**118**
7.1	Introduction	118
7.2	Database Selection, Preparation, and Baseline Characteristics	121
7.3	UNet Architectures	122
7.4	Methodology and Experiments	125
7.5	Results	126
7.6	Performance Evaluation	127
7.7	Discussion	135
7.8	Conclusion	138
7.9	Proposed Extension	138
8.0	**Localization of Common Carotid Artery Transverse Section in B-mode Ultrasound Images using Faster RCNN: A Deep Learning Approach**	**139**
8.1	Introduction	139
8.2	Common Carotid Artery Database	141
8.3	Methodology	142
8.4	Experimental protocols	146
8.5	Results	147
8.6	Discussion	148
8.7	Conclusion	149
9.0	**Conclusion and Future Scope**	**151**
9.1	Conclusion	151
9.2	Future Scope	152
	Appendix A	154
	References	155
	Author's List of Publications (on PhD Work)	169

List of Tables

Table No.	Description	Page No.
1.1	Sector-wise subjects of the articles studied in this Chapter	**04**
1.2	Biological Phenomenon of atherosclerosis disease	**09**
2.1	Deep learning UNet models for Biomedical Image Segmentation	**16**
2.2	CCA and ICA Plaque segmentation Deep learning techniques	**16**
2.3	cIMT segmentation Deep learning techniques	**21**
3.1	Hyper-parameters for experiments with SDL and HDL models	**35**
3.2	Results for five kinds of DL model using CE-loss function (Mean±SD)	**36**
3.3	Results for five kinds of DL model using DSC-loss (Mean±SD)	**36**
3.4	Jaccard *vs*. Dice performance for all five DL models using CE-loss (Mean±SD)	**39**
3.5	Jaccard *vs*. Dice performance for all five DL models using DSC-loss (Mean±SD)	**39**
3.6	AUC (*p*-values) for all DL models using CE-loss *vs*. DSC-loss	**40**
3.7	Correlation coefficient between GT area and estimated area for all DL models	**41**
3.8	Area error between AI and GT plaque for all DL models using CE and DSC-loss functions. (a) 80% of the database, (b) MAD	**43**
3.9	Benchmarking table in chronological order	**46**
3.10	Performance of the mean of five* AI models: CE-loss vs. DSC-loss	**47**
4.1	Baseline characteristics of the Japanese cohort	**56**
4.2	Mean performance parameters of UNet and SegNet-UNet AI models (all in %).	**63**
4.3	Performance parameters comparison of UNet, SegNet-UNet and AtheroEdge 2.0	**64**
4.4	Benchmarking table showing studies related to PA measurement	**70**
4.5	Benchmark studies related to TPA cut-off, granularity of risk, cohort type	**72**
4.6	Variation in AUC w.r.t. change in PA cut-off	**72**
5.1	Summary of all experiments performed on a multi-ethnic database	**79**
5.2	Classification parameters of the test dataset of all experiments	**80**
5.3	Performance and statistical parameters of the test dataset of all experiments	**81**
5.4	Comparison of experiments and validation of hypothesis	**86**
5.5	Benchmarking table showing multi-ethnic database studies for atherosclerotic plaque measurement	**86**

6.1	Hyperparameters And Model Sizes	**103**
6.2	CCA Plaque Segmentation Results	**104**
6.3	ICA Plaque Segmentation Results	**104**
6.4	Performance Parameters Of CCA And ICA Data Experiment	**106**
6.5	Benchmarking Table Comprising Recent Studies for PA Measurement Using Dl Models	**114**
6.6	Scientific Validation on Unknown Data	**114**
7.1	Number of trainable parameters in different parts of the UNet architectures	**124**
7.2	Segmentation performance (in %) of all UNet models using ICA database DB1	**126**
7.3	Segmentation performance (in %) of all UNet models using CCA database DB2X	**126**
7.4	Performance parameters of all UNet models for ICA and CCA database experiments	**131**
7.5	Paired-t-Test metrics for GTPA and estimated area by all UNet models for ICA database	**131**
7.6	Paired-t-Test metrics for GTPA and estimated area by all UNet models for CCA database	**135**
7.7	Benchmarking current research against previous studies	**137**
8.1	Validation data results for a mean 2000 epochs	**147**
8.2	Test data results of Toshiba's scanner data set of 433 images	**147**
8.3	Comparison of existing literature with the current study based on some parameters	**150**

List of Figures

Table No.	Description	Page No.
1.1	A schematic view of the atherogenesis	**03**
1.2	PRISMA Model for CVD risk biomarker measurement	**04**
1.3	Anatomy of the human cerebrovascular system. Atherosclerotic plaque growth in carotid arteries (left) unidirectional growth (right) bidirectional growth)	**06**
1.4	Carotid artery subsections CCA, ICA, and ECA in B-mode US image	**06**
1.5	Seven factors to avoid CVDs in life	**07**
2.1	Basic UNet architecture for carotid plaque segmentation	**14**
2.2	CCA Plaque area measurement in Japanese diabetic patients database (a) low (b) moderate risk and Hongkong database (c) low (d) moderate risk	**20**
2.3	ICA Plaque segmentation from moderate risk and high-risk patients' US image	**20**
2.4	cIMT segmentation in high-risk (left) and low-risk (right) CCA US images	**22**
2.5	Plaque classification into symptomatic and asymptomatic categories	**22**
3.1	Example of B-mode ICA US scans showing large plaque with black shadow	**26**
3.2	AtheroEdge™ 3.0. DL, HDL, ROC, CDP, CC, BA, CE-loss, and DSC-loss	**27**
3.3	(a) Raw and binary GT masks. R1 and R2 (high-plaque) and R3 and R4 (low-plaque) represent the raw ICA B-mode scans. Images marked G1, G2, G3, and G4 are the corresponding GT binary masks	**29**
3.4	Three SDL and two basic HDL segmentation models	**31-32**
3.5	Raw grayscale ICA image (top), AI-estimated binary mask using UNet with CE-loss function (middle), and GT binary mask (bottom)	**33**
3.6	Examples showing plaque segmentation in B-mode ICA and B-mode US images. Left: moderate-plaque. Right: high-plaque. The AI-based plaque region is shown in red, and the difference between AI and GT is shown in green colour. The yellow dotted regions show high curvature zones. Left image: A_{gt}=48.79 mm^2 A_{ai}=43.79 mm^2; (A_{gt}-A_{ai})=5.22 mm^2; Right image: A_{gt}=99.22 mm^2 A_{ai}=101.45 mm^2; (A_{gt}-A_{ai})=2.27 mm^2;	**35**
3.7	Estimated plaque area and difference area in (a), (b) (high-plaque), (c), (d) (low-plaque) images. Each (a), (b), (c), and (d) are divided into two columns	**37-38**

	consisting of CE-loss and DSC-loss. There are six rows: GT, UNet, UNet+, SegNet, SegNet-UNet, SegNet-UNet+	
3.8	Bar charts showing mean performance parameters and FoM for ten DL models	**41**
3.9	ROC curves for the sensitivity of the five models using CE-loss and DSC-loss.	**42**
3.10	CC between GT area and AI-estimated area for five models using CE-loss and DSC-loss.	**42**
3.11	Bland-Altman plots for GT area and AI-estimated area for five models using CE-loss and DSC-loss	**44**
3.12	Cumulative distribution curves for area error between AI-estimated plaque area and GT plaque area for all DL models. Left: CE-loss. Right: DSC-loss	**44**
3.13	Segmentation of images in 1X, 2X, and 3X databases using the UNet (CE) model	**49**
3.14	Optimized accuracy for augmented databases using (a) CE-loss and (b) DSC-loss. The best accuracy was obtained using the augmentation protocol for 2X	**49**
3.15	Examples showing positive remodelling	**51**
4.1	Online deep learning system (AtheroEdge 3.0) for high-risk plaque detection, quantification, and risk stratification	**55**
4.2	Schematic diagram of solo deep learning-based UNet architecture	**58**
4.3	Bridge network of the UNet architecture	**59**
4.4	Schematic diagram of hybrid deep learning-based SegNet-UNet architecture	**60**
4.5	Overlays of GT (white arrow) and AI (black arrow) plaque area of the CCA US. (a) Ground truth plaque only (white arrow) (b) UNet vs GT plaque (c) SegNet-UNet vs GT plaque. Gray colour arrows show the difference between GT and AI	**62**
4.6	Performance parameters of the UNet and SegNet-UNet models	**63**
4.7	Correlation of the three models: UNet (Black), SegNet-UNet (Red), and AtheroEdge 2.0 (Blue) against GT plaque area	**64**
4.8	Bland-Altman plots for (a) UNet (b) SegNet-UNet (c) AtheroEdge 2.0	**65**
4.9	Receiver Operating Characteristics and AUC for UNet, SegNet-UNet and AtheroEdge 2.0 for three kinds of PA Cut-offs (a) 38 mm^2 (b) 40 mm^2 (c) and 42 mm^2	**67**
4.10	Cumulative Distribution Frequency curve and area error threshold for 90% image database. (a) UNet: **9.9 mm^2** ; (b) SegNet-UNet: **8 mm^2**; (cc) AtheroEdge	**67**

	2.0: **9.6 mm²**	
4.11	Paired sample t-Test between (a) GT and UNet (b) GT and SegNet-UNet and (c) GT and AtheroEdge 2.0.	**68**
4.12	Wilcoxon test between (a) GT and UNet (b) GT and SegNet-UNet and (c) GT and AtheroEdge 2.0	**68**
5.1	System diagram for unseen data processing	**76**
5.2	Bar chart for all performance parameters of Unseen AI and Seen AI experiments	**80**
5.3	Generation of difference between the GT and AI overlay images	**81**
5.4	Visual results of the Unseen AI and Seen AI experiments	**82**
5.5	Regression plots for Unseen AI and Seen AI experiments	**82**
5.6	Receiver operating characteristics (ROC) curves and AUCs for the Unseen AI and Seen AI experiments	**83**
5.7	Bland–Altman's plots for Unseen and Seen experiments	**83**
5.8	Comparison of paired t-test curves for Unseen AI and Seen AI database experiments	**84**
5.9	Comparison of ANOVA test curves for Unseen AI and Seen AI database experiments	**84**
5.10	Comparison of ROC curve for unseen and seen database experiments	**85**
6.1	Global system for stroke risk assessment. The central engine is the automated segmentation using U-series architecture	**92**
6.2	Column 1 and column 2 are CCA scans while column 3 and column 4 are ICA scans. Row 1 is raw scans and row 2 is binary (mask) images used as ground truth	**93**
6.3	UNet architecture	**94**
6.4	UNet+ architecture	**95**
6.5	UNet++ Architecture	**95**
6.6	UNet3P architecture	**96**
6.7	Autoencoder architecture	**97**
6.8	Inception-UNet HDL architecture showing encoder-decoder phases	**98**
6.9	Squeeze-UNet HDL architecture with four fire models on the left (encoder) and four fire models on the right (decoder).	**99**
6.10	Fractal fundamental block used for designing Fractal-Unit architecture	**100**
6.11	Fractal-UNet architecture	**101**

6.12	Estimated (red) and the absolute difference between estimated and gold standard (green) plaque area in CCA and ICA images. Column 1: Moderate-plaque CCA; Column 2: Low-plaque CCA; Column 3: High-plaque ICA; Column 4: Moderate-plaque ICA. Row1: Binary mask; Row2: Ground truth region; Row 3: UNet; Row 4: UNet+; Row 5: UNet++; Row 6: Inception-UNet; Row 7: Fractal-UNet; Row 8: Squeeze-UNet.	**105**
6.13	CCA Regression curves between estimated PA of models vs. ground truth plaque area	**107**
6.14	ICA Regression curves between estimated PA of models vs. ground truth plaque area	**107**
6.15	Bland Altman's plot between CCA estimated PA of models vs. ground truth plaque area	**108**
6.16	Bland-Altman's plot between ICA estimated PA of models vs. ground truth plaque area	**108**
6.17	AUC for CCA analysis	**109**
6.18	AUC for ICA analysis	**109**
6.19	Bar chart showing model size, training time, and training parameters	**111**
7.1	Global system (under the class of AtheroEdge™ 3.0) of carotid plaque segmentation.	**120**
7.2	Attention block with input features, gating signals and weighted output	**123**
7.3	The attention gate mechanism between first encoder and decoder layer	**124**
7.4	Four-stage Attention-UNet model	**124**
7.5	Visual results of the segmentation of Japanese, Hong Kong and UK (ICA) databases, performed by UNet, UNet++, UNet3P, Fractal-UNet, Squeeze-UNet, and Attention-UNet models	**128**
7.6	Attention channel effect on plaque segmentation on critical images of moderate and high plaque	**129**
7.7	Regression plot for all UNet models for ICA DB1 databases	**130**
7.8	Regression Plot for all 6 types of UNet models for CCA DB2A database	**130**
7.9	ROC curves for all 6 types of UNet model for ICA DB1 database	**132**
7.10	ROC Plot for all 6 types of UNet models for CCA DB2A database	**132**
7.11	Paired samples t-Test Plot for all 6 types of UNet models for ICA DB1 databases	**133**

7.12	Paired samples t-Test Plot for all 6 types of UNet models for CCA DB2A database	**133**
7.13	Bland-Altman Plot of all 6 types of models for ICA DB1 database	**134**
7.14	Bland-Altman Plot of all 6 types of models for CCA DB2A database	**134**
7.15	Vision Transformer based segmentation results	**137**
8.1	Raw images of B-mode ultrasound of CCA transverse section obtained from (a) Ultrasonix scanner (b) Toshiba's scanner	**141**
8.2	Flowchart of FRCNN explaining the localization of artery in BUS images	**142**
8.3	Schematic diagram of object class detection with RPN as a combined network: FRCNN	**143**
8.4	Generation of the anchor boxes from convolutional feature map for each sliding window	**144**
8.5	FRCNN output of combined layer using Toshiba's scanner test data showing (a) correct bbox (b) multiple boxes (c) no bbox (d) wrong bbox, around the cross-section of the carotid artery with classification score	**148**
A.1	Hypertension vs. AI plaque area. Top right quadrant are 27 patients with high HT and PA>40 mm^2.	**154**
A.2	Smoking parameter Vs. AI plaque area. Top right quadrant are 8 smokers and PA>40 mm^2.	**154**
A.3	Family history relation Vs. AI plaque area. Top right quadrant are 5 studies with family history and PA>40 mm^2 .	**154**

List of Abbreviations

SN	Acronym	Description of the Acronyms
1	AI	Artificial Intelligence
2	ASE	American Society of Echocardiography
3	ADAM	Adaptive Learning Rate Optimization Algorithm
4	ADPA	Absolute Plaque Area Difference
5	AST	Artery Segment Type
6	AUC	Area Under the ROC Curve
7	BA	Bland-Altman's Plot
8	CAD	Computer-Aided Diagnosis
9	CC	Coefficient of Correlation
10	CCA	Common Carotid Artery
11	CDP	Cumulative Distribution Plot
12	CDC	Centre for Disease Control and Prevention
13	CE-loss	Cross Entropy Loss
14	cIMT	Carotid Intima Media Thickness
15	CNN	Convolutional Neural Network
16	CT	Computed Tomography
17	CV	Cross-Validation
18	CVDs/CVEs	Cardiovascular Diseases/Events
19	DL	Deep Learning
20	DLPA-CE	Deep learning Plaque Area using CE-loss
21	DLPA-DSC	Deep Learning Plaque Area using DSC-loss
22	DSC-loss	Dice Similarity Coefficient Loss
23	ECA	External Carotid Artery
24	ECST	European Carotid Surgery Trial
25	FCN	Fully Connected Network
26	GPU	Graphics Processing Unit
27	GSM	Grey Scale Median
28	GT	Ground Truth
29	GTPA	Ground Truth Plaque Area
30	HT	Hypertension
31	HDL	Hybrid Deep Learning, high density lipoprotein
32	HDLPA-CE	Hybrid Deep Learning Plaque Area using CE-loss
33	HDLPA-DSC	Hybrid Deep Learning Plaque Area using DSC-loss
34	ICA	Internal Carotid Artery
35	IMTV	Intima–Media Thickness Variability
36	LD	Lumen Diameter
37	LDL	Low Density Lipoprotein
38	LI	Lumen-Intima

39	MA	Media-Adventitia
40	MAD	Mean Absolute Difference
41	MCC	Mathew's Correlation Coefficients
42	MI	Myocardial Infraction
42	ML	Machine Learning
43	MPH	Maximum Plaque Height
44	MRI	Magnetic Resonance Imaging
45	MSE	Mean Squared Error
46	NASCET	North American Symptomatic Carotid Endarterectomy Trial
47	OCT	Optical Coherence Tomography
48	PA	Plaque Area
49	PTC	Plaque Tissue Characterization
50	PWV	Pulse Wave Velocity
51	ReLU	Rectified Linear Unit
52	RF	Resolution Factor
53	ROC	Receiver Operating Characteristics
54	SDL	Solo Deep Learning
55	SLFN	single-layer feed-forward network
56	SNR	signal-to-noise ratio
57	SOT	School of Thoughts
58	SPARC	Stroke Prevention and Atherosclerosis Research Centre (London, Canada)
59	TC	Total Cholesterol
60	TPA	Total Plaque Area
61	TPV	Total Plaque Volume
62	US	Ultrasound
63	WHO	World Health Organization

Symbol Table

SN	Symbol	Description of the symbols
1	L_{CE}	Cross Entropy-loss
2	L_{DSC}	Dice Similarity Coefficient-loss
3	m	*'m'* is index representing AI model number
4	n	*'n'* is for index representing image number in the database
5	$\bar{\mathcal{A}}_{ai}(m)$, $\bar{\alpha}_{ai}(m)$	Mean estimated plaque area for all images using AI model 'm'
6	$\mathcal{A}_{ai}(m,n)$, $\alpha_{ai}(m,n)$	Estimated plaque area using AI model 'm' and image 'n'
7	$\mathcal{A}_{gt}(n)$, $\alpha_{gt}(n)$	GT plaque area for image 'n'
8	$\bar{\mathcal{A}}_{gt}$, $\bar{\alpha}_{gt}$	Mean ground truth area for all images in the database
9	$FoM(m)$	Figure-of-Merit for model 'm'

10	JI	Jaccard Index
11	DSC	Dice Similarity Coefficient
12	N_p	Sample size computed using power analysis
13	MoE	Margin-of-Error for power analysis
14	z	Z-score from standard z-table for power analysis
15	TP,TN	True Positive and True Negative
16	FP, FN	False Positive and False Negative
17	y_i	GT label
18	a_i	SoftMax classifier probability
19	Y_p	Ground truth image symbol for DSC computation
20	$\widehat{Y_p}$	AI-estimated image symbol for DSC computation
21	P	Total number of pixels in an image in x,y direction
22	K10	Cross-validation protocol with 90% training and 10% testing
23	1.5X, 2X,	Augmented databases of sizes 1.5 and 2 folds, respectively
24	2.5X, 3X	Augmented databases of sizes 2.5 and 3 folds, respectively
25	Area_{gt}	Plaque area computed using Ground Truth envelope
26	Area_{ai}	Plaque area computed using AI model
27	S_{FM}	Size of feature matrix
28	W	Input Shape
29	K	Filter Shape
30	P	Padding
31	S	Stride
	Ten Deep Learning Segmentation Architectures	
32	UNet (CE)	'U' Shape based seg arch using CE-loss
33	SegNet (DSC)	Segm[#]. arch[%]. with reduced learning parameters using CE-loss
34	UNet+ (CE)	'U' Shape network with enhanced skip connections using CE-loss
35	SegNet-UNet (CE)	HDL model designed by fusing SegNet and UNet using CE-loss
36	SegNet-UNet+ (CE)	HDL model designed by fusing SegNet and UNet+ using CE-loss
37	UNet (DSC)	'U' Shape based segm. Arch. using DSC-loss
38	SegNet (DSC)	Segm[#]. arch[%]. with reduced learning parameters using DSC-loss
39	UNet+ (DSC)	'U' Shape network with enhanced skip connections using DSC-loss
40	SegNet-UNet (DSC)	HDL model designed by fusing SegNet and UNet using DSC-loss
41	SegNet-UNet+ (DSC)	HDL model designed by fusing SegNet and UNet+ using DSC-loss

[#]Segmentation; [%]Architecture